

# Specific Enzyme Complex of $\beta$ -1,4-Galactosyltransferase-II and Glucuronyltransferase-P Facilitates Biosynthesis of N-linked Human Natural Killer-1 (HNK-1) Carbohydrate\*<sup>[5]</sup>

Received for publication, February 21, 2011, and in revised form, July 5, 2011. Published, JBC Papers in Press, July 19, 2011, DOI 10.1074/jbc.M111.233353

Tetsuya Kouno<sup>‡</sup>, Yasuhiko Kizuka<sup>§1</sup>, Naoki Nakagawa<sup>‡</sup>, Toru Yoshihara<sup>¶||</sup>, Masahide Asano<sup>¶</sup>, and Shogo Oka<sup>‡2</sup>

From the <sup>‡</sup>Department of Biological Chemistry, Human Health Sciences, Graduate School of Medicine, and <sup>§</sup>Department of Biological Chemistry, Graduate School of Pharmaceutical Sciences, Kyoto University, Kyoto 606-8507 and the <sup>¶</sup>Division of Transgenic Animal Science, Advanced Science Research Center, and <sup>||</sup>Research Center for Child Mental Development, Kanazawa University, Kanazawa 920 8640, Japan

Human natural killer-1 (HNK-1) carbohydrate is highly expressed in the nervous system and is involved in synaptic plasticity and dendritic spine maturation. This unique carbohydrate, consisting of a sulfated trisaccharide (HSO<sub>3</sub>-3GlcA $\beta$ 1-3Gal $\beta$ 1-4GlcNAc-), is biosynthesized by the successive actions of  $\beta$ -1,4-galactosyltransferase ( $\beta$ 4GalT), glucuronyltransferase (GlcAT-P and GlcAT-S), and sulfotransferase (HNK-1ST). A previous study showed that mice lacking  $\beta$ 4GalT-II, one of seven  $\beta$ 4GalTs, exhibited a dramatic loss of HNK-1 expression in the brain, although  $\beta$ 4GalT-I-deficient mice did not. Here, we investigated the underlying molecular mechanism of the regulation of HNK-1 expression. First, focusing on a major HNK-1 carrier, neural cell adhesion molecule, we found that reduced expression of an N-linked HNK-1 carbohydrate caused by a deficiency of  $\beta$ 4GalT-II is not likely due to a general loss of the  $\beta$ 1,4-galactose residue as an acceptor for GlcAT-P. Instead, we demonstrated by co-immunoprecipitation and endoplasmic reticulum-retention analyses using Neuro2a (N2a) cells that  $\beta$ 4GalT-II physically and specifically associates with GlcAT-P. In addition, we revealed by pull-down assay that Golgi luminal domains of  $\beta$ 4GalT-II and GlcAT-P are sufficient for the complex to form. With an *in vitro* assay system, we produced the evidence that the kinetic efficiency  $k_{cat}/K_m$  of GlcAT-P in the presence of  $\beta$ 4GalT-II was increased about 2.5-fold compared with that in the absence of  $\beta$ 4GalT-II. Finally, we showed that co-expression of  $\beta$ 4GalT-II and GlcAT-P increased HNK-1 expression on various glycoproteins in N2a cells, including neural cell adhesion molecule. These results indicate that the specific enzyme complex of  $\beta$ 4GalT-II with GlcAT-P plays an important role in the biosynthesis of HNK-1 carbohydrate.

Glycosylation is a major post-translational modification, especially for cell surface and extracellular proteins, and plays important roles in cellular functions such as adhesion, endocytosis, and receptor signaling (1, 2). In general, glycan is biosynthesized in a stepwise manner by ER<sup>3</sup>- or Golgi-resident glycosyltransferases. As most of these glycosyltransferases have been cloned, there is an overall understanding of the pathway of production. However, the expression of a given glycosyltransferase does not always reflect that of its product, because it has become clear that activities of glycosyltransferases are regulated by oligomerization or proteolytic cleavage (3, 4). In addition, some glycosyltransferases form heterocomplexes that alter their activities, substrate specificity, or distribution in the ER or Golgi apparatus (5, 6). Thus, to understand the functions and biosynthesis of glycans, it is necessary to clarify how the activity of individual glycosyltransferases is regulated in cells.

Human natural killer-1 (HNK-1) carbohydrate is highly expressed on several cell adhesion molecules in the nervous system, including the neural cell adhesion molecule (NCAM) (7, 8). HNK-1 carbohydrate has a unique structure, including a sulfated trisaccharide (HSO<sub>3</sub>-3GlcA $\beta$ 1-3Gal $\beta$ 1-4GlcNAc-) (9, 10), and is biosynthesized by the successive actions of  $\beta$ -1,4-galactosyltransferase ( $\beta$ 4GalT), a glucuronyltransferase (GlcAT-P or GlcAT-S), and a sulfotransferase (HNK-1ST) (11–13). We previously generated mice lacking the gene for GlcAT-P, a major glucuronyltransferase in the nervous system (14). The GlcAT-P-deficient mice showed an almost complete loss of HNK-1 expression in the brain and exhibited reduced long term potentiation at hippocampal CA1 synapses along with impaired maturation of dendritic spines, indicating an important role for this glycan in synaptic plasticity (14, 15). In terms of the expression, we have been uncovering well controlled mechanisms of HNK-1 biosynthesis. For instance, GlcAT-P (S) and HNK-1ST form a functional complex, and the distribution of GlcAT-P in the Golgi is regulated by a small GTPase (16). However, it is still unclear how the inner N-acetyllactosamine structure (Gal $\beta$ 1-4GlcNAc) for HNK-1 carbohydrate is synthesized and how HNK-1 is selectively attached to limited kinds of carrier proteins.

\* This work was supported in part by Grant-in-aid for Scientific Research (B) 21370053 (to S. O.) from the Ministry of Education, Culture, Sports, Science and Technology and in part by the Ministry of Health, Labor, and Welfare of Japan Health and Labour Sciences Research Grant on Comprehensive Research on Disability Health and Welfare, H21-012.

<sup>[5]</sup> The on-line version of this article (available at <http://www.jbc.org>) contains supplemental Figs. 1–3.

<sup>1</sup> Present address: Disease Glycomics Team, Systems Glycobiology Research Group, Advanced Science Institute, RIKEN, Saitama 351-0198, Japan.

<sup>2</sup> To whom correspondence should be addressed: Kawahara-cho 53, Shogoin, Sakyo-ku, Kyoto 606-8507, Japan. Tel./Fax: 81-75-751-3959; E-mail: shogo@hs.med.kyoto-u.ac.jp.

<sup>3</sup> The abbreviations used are: ER, endoplasmic reticulum;  $\beta$ 4GalT,  $\beta$ 1,4-galactosyltransferase; GlcAT, glucuronyltransferase; HNK-1, human natural killer-1; PSA, polysialic acid; PST, polysialyltransferase; NCAM, neural cell adhesion molecule; ASOR, asialo-orosomucoid.

## Complex of $\beta$ 4GalT-II and GlcAT-P in HNK-1 Biosynthesis

Although the  $\beta$ 4GalT family is known to have seven members ( $\beta$ 4GalT-I to VII) *in vivo* (17, 18), the biological role of each is not fully understood. Some of them are able to synthesize *N*-acetylglucosamine on glycoproteins, which is potentially further modified by GlcAT-P. We recently reported that  $\beta$ 4GalT-II-deficient mice showed similar phenotypes to GlcAT-P-deficient mice with a reduction in HNK-1 expression and impaired spatial learning and memory (19), although HNK-1 expression was unaltered in the  $\beta$ 4GalT-I-deficient mouse brain (20) despite the similarity in primary structure and acceptor specificity of these two enzymes (21, 22). These results indicated that  $\beta$ 4GalT-II has specific roles in the biosynthesis of HNK-1 carbohydrate. However, the precise molecular mechanism has not been explored.

Polysialic acid (PSA), a well known neural specific glycan, plays crucial roles in the development of the nervous system, attenuating cellular interactions because of its large and highly negative charge (23, 24). PSA has features in common with HNK-1 in that it is mainly expressed on NCAM and has an *N*-acetylglucosamine residue (Gal $\beta$ 1-4GlcNAc-) in its backbone structure synthesized by  $\beta$ 4GalT (25). Surprisingly, however,  $\beta$ 4GalT-II-deficient mice as well as  $\beta$ 4GalT-I-deficient mice expressed PSA at the same level as wild-type mice (19, 20), indicating the biosynthesis of HNK-1 and PSA to be more complicated mechanisms than was previously thought.

In this study, we demonstrated that  $\beta$ 4GalT-II but not  $\beta$ 4GalT-I physically interacts with GlcAT-P but not with a polysialyltransferase (PST), which explains the loss of or remaining expression of HNK-1 or PSA in these knock-out mice. Furthermore, overexpression of  $\beta$ 4GalT-II enhanced HNK-1 biosynthesis by GlcAT-P compared with  $\beta$ 4GalT-I, suggesting that  $\beta$ 4GalT-II is specifically required for production of HNK-1.

### EXPERIMENTAL PROCEDURES

**Materials**—The monoclonal antibody (mAb) M6749 against HNK-1 carbohydrate was a gift from Dr. H. Tanaka (Kumamoto University). HNK-1 mAb was purchased from the American Type Culture Collection. The rat anti-mouse NCAM mAb (clone H28) was kindly provided by Dr. K. Ono (Kyoto Prefectural University). RCA120 was purchased from Seikagaku Corp., Tokyo, Japan. The mouse anti-FLAG M2 mAb and rabbit anti-FLAG polyclonal antibody (pAb) were obtained from Sigma. The mouse anti-Myc mAb and rabbit anti-Myc pAb were from Millipore and Abcam, respectively. The rabbit anti-GlcAT-P pAb (GP2) was generated as described previously (16). The mouse anti-GM130 mAb was purchased from BD Biosciences. HRP-conjugated anti-mouse IgG, anti-mouse IgM, anti-rabbit IgG, and anti-rat IgG were obtained from Invitrogen. Protein G-Sepharose TM4 Fast Flow and IgG-Sepharose TM6 Fast Flow were from GE Healthcare. The expression vector pcDNA3.1/myc-His B was from Invitrogen, and p3 $\times$ FLAG-CMV-10 and p3 $\times$ FLAG-CMV-14 were from Sigma. The plasmid pEF-BOS was kindly provided by Dr. S. Nagata (Kyoto University).

**Mice**— $\beta$ 4GalT-I-deficient mice and  $\beta$ 4GalT-II-deficient mice were generated as described previously (19, 26).  $\beta$ 4GalT-II-deficient mice backcrossed to C57BL/6 mice for more than

10 generations were used for the experiments, whereas  $\beta$ 4GalT-I-deficient mice on a mixed background of 129/Sv and C57BL/6 were used because the mice with the C57BL/6 background were lethal.<sup>4</sup> The animal experiments were conducted according to the Fundamental Guidelines for Proper Conduct of Animal Experiments and Related Activities in Academic Research Institutions under the jurisdiction of the Ministry of Education, Culture, Sports, Science and Technology of Japan and approved by the Committees on Animal Experimentation of Kanazawa University and Kyoto University.

**Preparation of Brain Homogenate and Membrane Fraction**—Whole brains from 4-week-old mice were homogenized with a Polytron homogenizer in 9 volumes of 50 mM Tris-HCl, pH 7.4, containing 150 mM NaCl, 1 mM EDTA, and protease inhibitors (Nacalai Tesque, Kyoto, Japan). The homogenate was centrifuged at 1,000  $\times$  *g* for 10 min at 4 °C to remove the nuclei and then centrifuged again at 105,000  $\times$  *g* for 1 h at 4 °C. The resulting pellet was used as the membrane fraction.

**Peptide *N*-Glycosidase F Digestion**—The membrane fraction of mouse brain was dissolved and denatured with phosphate-buffered saline (PBS) containing 0.5% SDS, 1% 2-mercaptoethanol, and 20 mM EDTA. To reduce the concentration of SDS, the sample was diluted with 4 volumes of PBS containing 0.5% Triton X-100. Two units of peptide *N*-glycosidase F (Roche Applied Science) were added, and the solution was incubated for 16 h at 37 °C.

**Expression Plasmids**—The subcloning of rat GlcAT-P cDNA into pEF-BOS was performed as described previously (11). The expression plasmid for GlcAT-P-AAA (pEF-BOS/GlcAT-P-AAA) was constructed as reported (16). The mouse  $\beta$ 4GalT-I and  $\beta$ 4GalT-II coding sequences were amplified by PCR using the primers listed below to create HindIII and EcoRV (skipping stop codon) sites and then cloned into pcDNA3.1/myc-His B. The mouse PST coding sequence was cloned into p3 $\times$ FLAG-CMV-14 as described previously (16). The expression plasmid for PST-AAA-FLAG (p3 $\times$ FLAG-CMV-14/PST-AAA) was constructed as follows. p3 $\times$ FLAG-CMV-14/PST-AER-FLAG was constructed using QuikChange Lightning site-directed mutagenesis kits (Stratagene) according to the manufacturer's directions using the primers listed below, with p3 $\times$ FLAG-CMV-14/PST-FLAG as a template. Then, p3 $\times$ FLAG-CMV-14/PST-AAA-FLAG was constructed as mentioned above using the primers listed below, with p3 $\times$ FLAG-CMV-14/PST-AER-FLAG as a template. cDNAs encoding the Golgi luminal domains of mouse  $\beta$ 4GalT-I and -II (from Ser-43 and Asp-33 to the C terminus) were amplified by PCR using the primers listed below and cloned into pEF-BOS-protein A (27), which contains the insulin signal sequence and IgG-binding domain of protein A. For the constructions of prot.A-GalT-Icat and -IIcat, cDNAs encoding the catalytic domains of mouse  $\beta$ 4GalT-I and -II (from Leu-128 and Ile-91 to the C terminus) (28) were amplified by PCR using the primers listed below and cloned into pEF-BOS-protein A. pEF-BOS-protein A was digested with SmaI. Then the blunt end fragments of  $\beta$ 4GalTs were cloned. GlcAT-P-sol was amplified by PCR using the primers listed

<sup>4</sup> M. Asano and N. Hashimoto, unpublished results.

below with pEF-BOS/GlcAT-P as a template to create EcoRV and NotI sites, and cloned into pEF-1/V5-His A into which the signal sequence of insulin had been inserted between EcoRI and EcoRV sites.

The primers used for  $\beta$ 4GalT-I-myc were as follows: GGG-AAGCTTGC GGCCGTCTCTCAGCCG and TCTCGGTGTCCCGATGTCCACTGTG;  $\beta$ 4GalT-II-myc, GGGAAGCTTCTTGC GGCGATGAGCAGACTG and GCCTTGAGTGA-GCCACGAGA; PST-AER-FLAG, ATGCGCTCAATTGCAG-AACGGTGGACCATCTGCACTATAAGTC and GACTTATAGTGCAGATGGTCCACCGTTCTGCAATTGAGCGCAT; PST-AAA-FLAG, ATGCGCTCAATTGCAGCAGCGTGGACCATCTGCACTATAAGTC and GACTTATAGTGCAGATGGTCCACCGCTGCTGCAATTGAGCGCAT; prot.A-GalT-I (Ser-43), CTGGCCGCGATCTGAGCCG and CTATCTCGGTGTCCCGATGTCCACT; prot.A-GalT-II (Asp-33), ACGTCTATGCCAGCACCTGG and TCAGCCTTGAGTGAGCCACGACATG; prot.A-GalT-Icat (Leu-128), TGCCAGCTTGCCCTGAGGAG and CTATCTCGGTGTCCCGATGTCCACT; prot.A-GalT-Iicat (Ile-91), TCATTCCGCCCTGTCCTGAC and TCAGCCTTGAGTGAGCCACGACATG; and GlcAT-P-sol, CCCC GCCATGAGGCACCACC and TGAGCGGCCGCTCAGATCTCCACCGAGGGGT.

**Cell Culture and Transfection**—N2a cells were cultured in minimum Eagle's medium supplemented with 10% fetal bovine serum at 37 °C until 50–70% confluent. For transfection, cells were plated on 60-mm tissue culture dishes, grown overnight, and then transfected with various expression constructs using FuGENE 6 (Roche Applied Science) according to the manufacturer's directions. Briefly, a 2.5 volume of FuGENE 6 and 1  $\mu$ g of each DNA were incubated with 100  $\mu$ l of minimum Eagle's medium for 15 min at room temperature, and then the mixture was added to the tissue culture dishes.

**Cell Lysis and Immunoprecipitation of Transiently Expressed Proteins**—Cells were collected 24 h after transfection and lysed with a buffer consisting of 20 mM Tris-HCl, pH 7.4, 150 mM NaCl, 1 mM EDTA, 1% Triton X-100, and a protease inhibitor mixture (Nacalai Tesque). After centrifugation, the clarified lysate was incubated with the anti-FLAG rabbit pAb or anti-Myc rabbit pAb for 0.5 h. The mixture was then incubated with protein G-Sepharose TM4 Fast Flow for 2 h with gentle shaking. The beads were precipitated by centrifugation (500  $\times$  g for 1 min) and washed three times with an excess volume of wash buffer consisting of 20 mM Tris-HCl, pH 7.4, 150 mM NaCl, and 0.1% Tween 20. Proteins bound to the Sepharose beads were eluted by boiling in Laemmli sample buffer.

**Immunostaining of N2a Cells**—At 24 h post-transfection, cells were washed with PBS, fixed with ice-cold methanol, and incubated with primary antibodies followed by Alexa Fluor-conjugated secondary antibodies (Invitrogen). Cells were visualized with a Fluoview laser confocal microscope system (Olympus).

**SDS-PAGE and Western Blot and Lectin Blot Analyses**—Proteins were separated by SDS-PAGE with the buffer system of Laemmli and transferred to nitrocellulose membranes. For Western blotting, after being blocked with 5% skim milk in PBS containing 0.05% Tween 20, the membrane was incubated with primary antibodies followed by HRP-conjugated secondary

antibodies. For lectin blotting, after being blocked with PBS containing 0.05% Tween 20 (T-PBS), the membrane was incubated with sialidase (Roche Applied Science) according to the manufacturer's instructions, and then incubated with HRP-conjugated lectin in T-PBS. Protein bands were detected with ECL (Pierce) using a LAS3000 Luminoimage analyzer (Fujifilm).

**Pulldown Assays**—N2a cells were transiently transfected with prot.A-GalT-I (Ser-43), -Icat (Leu-128), -II (Asp-33), or -Iicat (Ile-91) and GlcAT-P-sol. After 6 h of incubation, the culture medium was replaced with serum-free Opti-MEM 1 (Invitrogen) and incubation continued for another 2 days. Normal human IgG-conjugated Sepharose beads were added to the culture medium containing secreted proteins. The beads were precipitated by centrifugation (500  $\times$  g for 1 min) and then washed three times with an excess volume of wash buffer consisting of 20 mM Tris-HCl, pH 7.4, 150 mM NaCl, and 0.1% Tween 20. Proteins bound to the Sepharose beads were eluted by boiling in Laemmli sample buffer.

**Preparation of Protein A-fused GalTs**—COS-1 cells plated on 175-cm<sup>2</sup> tissue culture flasks were transfected with prot.A-GalT-I (Ser-43) or prot.A-GalT-II (Asp-33) using FuGENE 6 transfection reagent. After 5 h of incubation, the culture medium was replaced with serum-free ASF104 medium (Ajinomoto), followed by incubation for another 3 days. Then, the culture medium containing secreted proteins was applied to IgG-Sepharose TM6 fast flow column (GE Healthcare). Unbound proteins were washed out with more than 10 column volumes of PBS. Bound proteins were eluted with 100 mM glycine-HCl, pH 2.5, and then the eluate was immediately neutralized with 3 M Tris-HCl, pH 8.0. The purified prot.A-GalTs were used for the following kinetic analysis of GlcAT-P.

**Measurement of Glucuronyltransferase Activity**—The FLAG-tagged GlcAT-P catalytic domain (FLAG-P) used was expressed in *Escherichia coli* and purified as described previously (29). The enzymatic activity of GlcAT-P toward glycoprotein acceptors was measured according to the procedure described previously (10) with slight modification. In brief, prior to the assay, FLAG-P (25 ng) was incubated in the absence or presence of prot.A-GalT-I (Ser-43) or prot.A-GalT-II (Asp-33) (100 ng each) at room temperature for 15 min. The preincubated enzyme solution was added to a reaction mixture with a final volume of 25  $\mu$ l consisting of 200 mM MES, pH 6.5, 0.2% Nonidet P-40, 20 mM MnCl<sub>2</sub>, 0.1–20  $\mu$ g ASOR, 100  $\mu$ M UDP-[<sup>14</sup>C]GlcA (100,000 dpm), and 0.5 mM ATP. After incubation at 37 °C for 2 h, the assay mixture was spotted onto a Whatman No. 1 filter paper. The filter paper was washed with a 10% (w/v) trichloroacetic acid solution three times, followed by with ethanol/ether (2:1, v/v), and then with ether. The filter paper was air-dried, and then the radioactivity of [<sup>14</sup>C]GlcA-ASOR was counted with a liquid scintillation counter.

## RESULTS

**Unaltered Expression of N-Acetylglucosamine on a Major HNK-1 Carrier in  $\beta$ 4GalT-II-deficient Mice**—Recently, we reported that HNK-1 expression is substantially reduced in  $\beta$ 4GalT-II-deficient mice, although an earlier study revealed that  $\beta$ 4GalT-I-deficient mice expressed normal levels of

## Complex of $\beta 4\text{GalT-II}$ and $\text{GlcAT-P}$ in $\text{HNK-1}$ Biosynthesis

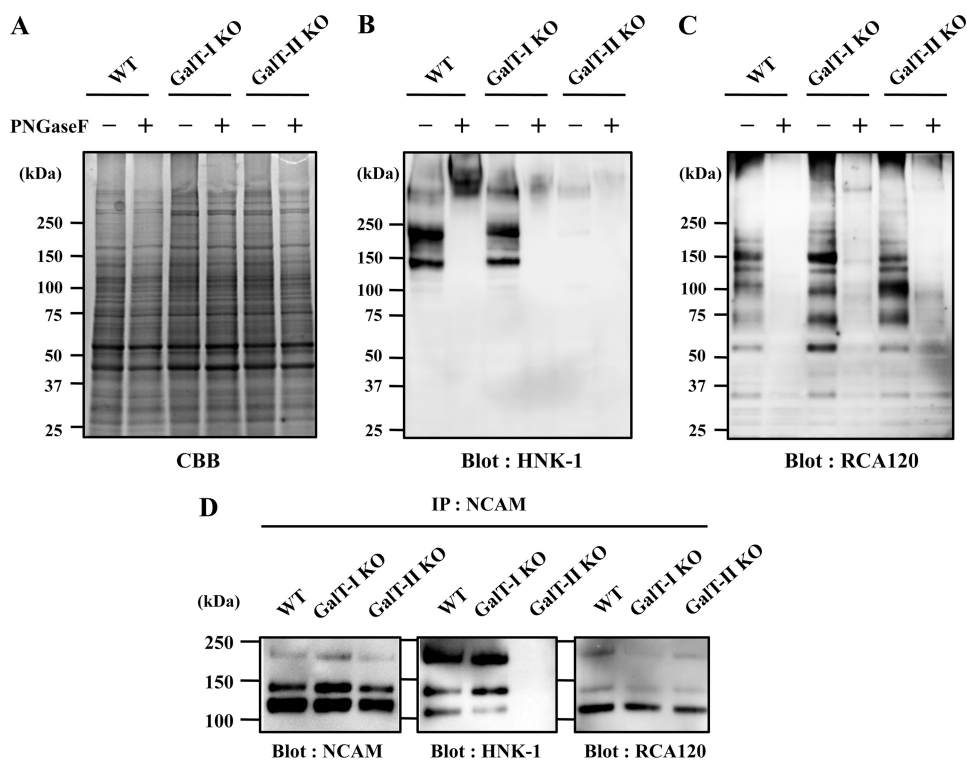


**FIGURE 1. Expression of HNK-1 carbohydrate and *N*-acetylglucosamine in mouse brains.** Membrane fractions of 4-week-old C57BL/6 (WT),  $\beta 4\text{GalT-I}$ -deficient (GalT-I-KO), and  $\beta 4\text{GalT-II}$ -deficient (GalT-II-KO) mouse brain were subjected to SDS-PAGE followed by Coomassie Brilliant Blue (CBB) staining (A), Western blotting with HNK-1 mAb (B), or lectin blotting with RCA120 (C). D, membrane fractions of 4-week-old mouse brains were immunoprecipitated (IP) with anti-NCAM antibody, subjected to SDS-PAGE, and blotted with anti-NCAM mAb, HNK-1 mAb, and RCA120. PNGase F, peptide:*N*-glycosidase F.

HNK-1 (19, 20). To directly compare the expression of HNK-1 in these mutant mice, brain membrane fractions were prepared from wild-type and  $\beta 4\text{GalT-I}$ , II-deficient mice (Fig. 1A) and Western-blotted with the HNK-1 mAb (Fig. 1B). Consistent with previous reports, HNK-1 expression was dramatically decreased in  $\beta 4\text{GalT-II}$ -deficient mice but was normal in  $\beta 4\text{GalT-I}$ -deficient mice. Most HNK-1 epitopes in the wild-type mice disappeared after treatment with peptide *N*-glycosidase F (Fig. 1B, 2nd lane), indicating that HNK-1 carbohydrates are mainly expressed on *N*-glycan in the membrane fraction. This suggests that  $\beta 4\text{GalT-II}$  synthesizes most HNK-1 carbohydrates on *N*-glycans in the brain. To explore the molecular mechanism involved, we first confirmed that the  $\text{GlcAT-P}$  transcript was expressed normally in these knock-out mice brains (supplemental Fig. 1). Next, to examine whether the *N*-acetylglucosamine residue remains in these knock-out mice, a lectin blot analysis was performed using RCA120, which predominantly recognizes the  $\beta$ Gal residue of *N*-acetylglucosamine. Because the nonreducing end of *N*-acetylglucosamine is often capped by sialic acid, the membrane was treated with sialidase prior to RCA120 blotting. As a result,  $\beta 4\text{GalT-I}$  and -II-deficient mice showed similar reactivity for RCA120 to wild-type mice, most of which disappeared after peptide *N*-glycosidase F treatment, indicating that the *N*-acetylglucosamine on *N*-glycans was normally expressed in these knock-out mice and that several  $\beta 4\text{GalTs}$  contribute to the biosynthesis of *N*-linked *N*-acetylglucosamine in the brain. This excludes the possibility that the reduction in HNK-1 is due to a general loss of *N*-acetylglucosamine in the  $\beta 4\text{GalT-II}$ -deficient brain.

Another possibility is that  $\beta 4\text{GalT-II}$  is the only  $\beta 4\text{GalT}$  in HNK-1-expressing cell or a specific  $\beta 4\text{GalT}$  for HNK-1 carrier proteins. To test this, we focused on NCAM. Because NCAM is a major carrier of HNK-1 carbohydrates in the nervous system, it must be expressed in HNK-1-positive cells. NCAM was immunoprecipitated from the brain membrane fraction and blotted with anti-NCAM mAb, HNK-1 mAb, and RCA120. As shown in Fig. 1D, three major splicing isoforms of NCAMs (NCAM-120, NCAM-140, and NCAM-180) are detected, and no difference in expression levels of each NCAM isoform (Blot: NCAM) or in reactivity with *Ricinus communis* agglutinin (Blot: *R. communis* agglutinin was observed among three genotypes). In contrast, HNK-1 is predominantly expressed on NCAM-180 and NCAM-140 rather than on NCAM120 in wild-type mice brain, which is consistent with a previous report (30). The HNK-1 on NCAM disappeared in  $\beta 4\text{GalT-II}$ -deficient mice (Blot: HNK-1). These results indicate that other  $\beta 4\text{GalTs}$  synthesize *N*-acetylglucosamine even onto NCAM in  $\beta 4\text{GalT-II}$ -deficient mice and also suggest that  $\beta 4\text{GalT-II}$  is not the only enzyme in HNK-1-expressing cells and not responsible for the general production of *N*-acetylglucosamine on HNK-1 carrier molecules. Therefore, it is possible that  $\text{GlcAT-P}$  transfers glucuronic acid (GlcA) only to the *N*-acetylglucosamine structure that  $\beta 4\text{GalT-II}$  synthesizes, prompting us to speculate that  $\text{GlcAT-P}$  specifically associates with  $\beta 4\text{GalT-II}$ .

**Co-immunoprecipitation of  $\text{GlcAT-P}$  and  $\beta 4\text{GalT-II}$** —To investigate the interaction between  $\beta 4\text{GalT-II}$  and  $\text{GlcAT-P}$ , we performed co-immunoprecipitation experiments. Myc-tagged  $\beta 4\text{GalT-I}$  or -II ( $\beta 4\text{GalT-I-myc}$  or  $\beta 4\text{GalT-II-myc}$ ) and

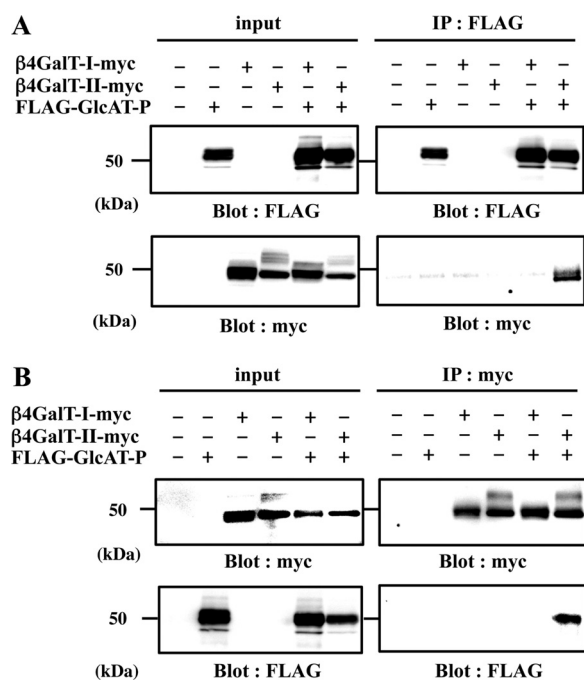


**FIGURE 2. Co-immunoprecipitation of GlcAT-P and  $\beta 4\text{GalT-II}$  in N2a cells.** Lysate of N2a cells transiently expressing FLAG-GlcAT-P,  $\beta 4\text{GalT-I-myc}$ , or  $\beta 4\text{GalT-II-myc}$  was immunoprecipitated (IP) with anti-FLAG pAb (A, IP: FLAG) or anti-Myc pAb (B, IP: myc), subjected to SDS-PAGE, and Western-blotted (Blot) with anti-FLAG mAb or anti-Myc mAb. To examine the level of each protein, the cell lysates were directly subjected to SDS-PAGE and Western blotting with anti-FLAG mAb or anti-Myc mAb (input).

FLAG-tagged GlcAT-P (FLAG-GlcAT-P) were transiently expressed in N2a cells, and cell lysates were incubated with anti-FLAG pAb to precipitate FLAG-GlcAT-P (Fig. 2A, IP: FLAG). Subsequent Western blotting was conducted with anti-Myc mAb to detect  $\beta 4\text{GalT-I}$  and -II-myc. As shown in Fig. 2A, right lower panel,  $\beta 4\text{GalT-II-myc}$  was co-immunoprecipitated by FLAG-GlcAT-P, whereas  $\beta 4\text{GalT-I-myc}$  was not. To determine whether FLAG-GlcAT-P could be conversely co-precipitated by  $\beta 4\text{GalT-II-myc}$ , we conducted immunoprecipitation using anti-Myc pAb. As shown in Fig. 2B, right lower panel, FLAG-GlcAT-P was co-immunoprecipitated by  $\beta 4\text{GalT-II-myc}$ , but not by  $\beta 4\text{GalT-I-myc}$ . These results revealed that GlcAT-P specifically interacted with  $\beta 4\text{GalT-II}$  in cells.

**Effect of ER-retained GlcAT-P on  $\beta 4\text{GalT-II}$  Localization—**Next, we performed an ER-retention assay (6, 31) to visualize the interaction. Normally, GlcAT-P and  $\beta 4\text{GalT-I}$  and -II mainly occur in Golgi, as was confirmed by co-localization with a Golgi marker, GM130, in N2a cells (supplemental Fig. 2). GlcAT-P appeared to co-localize with  $\beta 4\text{GalT-I}$  as well as  $\beta 4\text{GalT-II}$  under normal conditions (Fig. 3, B–G). In the ER-retention assay, we employed an ER-retained version of GlcAT-P in which a dibasic motif (K/R)(X)(K/R) was mutated (Fig. 3A). Some glycosyltransferases have this motif in their cytoplasmic tail, which is required for transport from the ER to the Golgi apparatus (32). Actually, GlcAT-P lacking this motif (GlcAT-P-AAA) was retained in the ER (Fig. 3, H and K, and also see supplemental Fig. 3, A and D) (16). To investigate the effect of GlcAT-P-AAA on the distribution of  $\beta 4\text{GalT-I}$  and -II, N2a cells expressing GlcAT-P-AAA and  $\beta 4\text{GalT-I}$  or -II-myc were immunostained. As a result, the location of  $\beta 4\text{GalT-II-myc}$

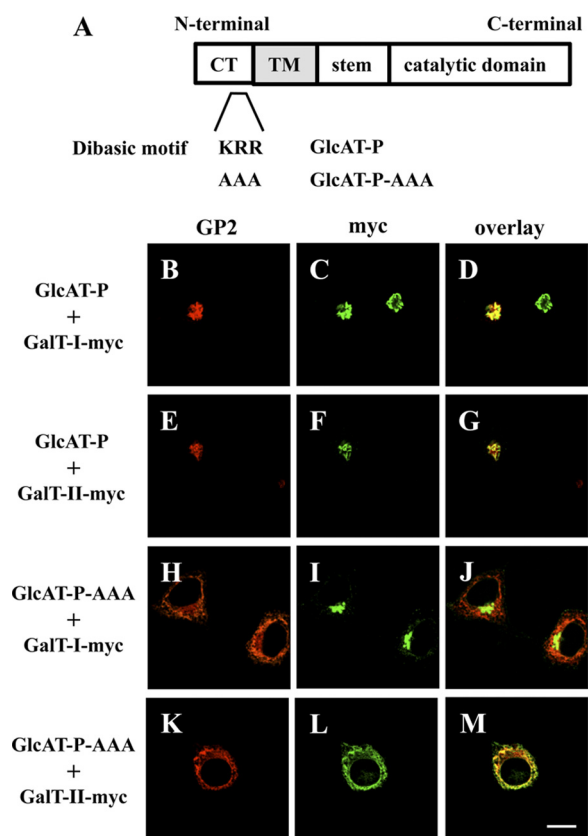


**FIGURE 3. ER retention assays using GlcAT-P-AAA.** A, schematic diagrams of GlcAT-P and GlcAT-P-AAA. CT, cytoplasmic tail, TM, transmembrane domain. B–M, N2a cells were transiently co-transfected with GlcAT-P or GlcAT-P-AAA and  $\beta 4\text{GalT-I-myc}$  or  $\beta 4\text{GalT-II-myc}$ . GlcAT-P and GlcAT-P-AAA were detected with GP2 pAb (B, E, H, and K) and Alexa 546-conjugated secondary antibodies.  $\beta 4\text{GalT-myc}$  (I and II) was detected with anti-Myc mAb (C, F, I, and L) and Alexa 488-conjugated secondary antibodies. D, G, J, and M, overlaid images. Bar, 10  $\mu\text{m}$ .

changed to the ER from the Golgi (Fig. 3L and supplemental Fig. 3E), which overlapped with GlcAT-P-AAA (Fig. 3M and supplemental Fig. 3F), whereas  $\beta 4\text{GalT-I-myc}$  was still localized to the Golgi regardless of the expression of GlcAT-P-AAA (Fig. 3, I and J, and also see supplemental Fig. 3, B and C). These results reinforce the notion of selective interaction between GlcAT-P and  $\beta 4\text{GalT-II}$  in cells.

**$\beta 4\text{GalT-II}$  and  $\beta 4\text{GalT-I}$  Do Not Associate with PST—**To examine the specificity of the binding between  $\beta 4\text{GalT-II}$  and GlcAT-P, we used a PST instead of GlcAT-P. PST is one of the  $\alpha 2,8$ -polysialyltransferases involved in the biosynthesis of PSA (33, 34), and PSA is attached to monosialylated *N*-acetylglucosamine on NCAM (35). Our previous study revealed that PSA was expressed in the brain of  $\beta 4\text{GalT-II}$ -deficient mice at the same level as in wild-type mice (19). This is also the case in  $\beta 4\text{GalT-I}$ -deficient mice (20). Therefore, we expected that  $\beta 4\text{GalT-I}$  and -II would not associate with PST.  $\beta 4\text{GalT-I}$ - or -II-myc and PST-FLAG were expressed in N2a cells, immunoprecipitated with anti-FLAG pAb, and subjected to Western blotting with anti-Myc mAb. As shown in Fig. 4, lower panel,  $\beta 4\text{GalT-I}$  and -II were not co-precipitated with PST, suggesting that these enzymes do not interact in cells.

To support the immunoprecipitation data, an ER retention assay was performed using PST-AAA-FLAG (Fig. 5A), a mutant

## Complex of $\beta 4\text{GalT-II}$ and $\text{GlcAT-P}$ in $\text{HNK-1}$ Biosynthesis

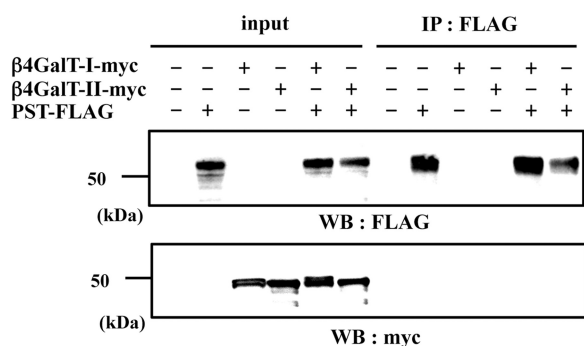


**FIGURE 4. Immunoprecipitation using PST-FLAG and  $\beta 4\text{GalT-myc}$  in N2a cells.** Lysate of N2a cells transiently expressing PST-FLAG,  $\beta 4\text{GalT-I-myc}$ , or  $\beta 4\text{GalT-II-myc}$  were immunoprecipitated (IP) with anti-FLAG pAb (IP: FLAG), subjected to SDS-PAGE, and Western-blotted with anti-FLAG mAb or anti-Myc mAb. To examine the level of each protein, the cell lysates were directly subjected to SDS-PAGE and then Western blotting (WB) with anti-FLAG mAb or anti-Myc mAb (input).

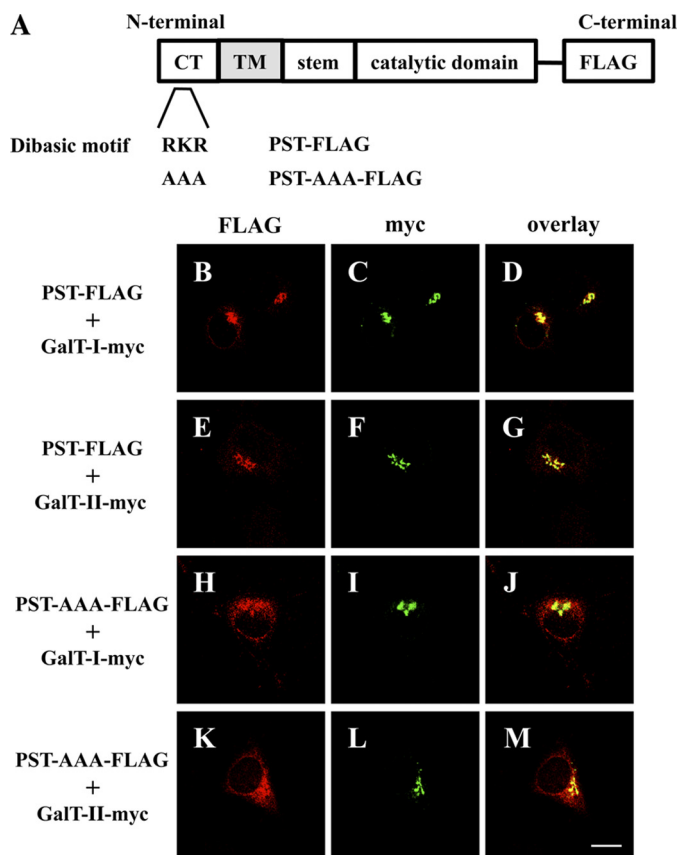


**FIGURE 5. ER retention assays using PST-AAA-FLAG.** A, schematic diagrams of PST-FLAG and PST-AAA-FLAG. B–M, N2a cells were transiently co-transfected with PST-FLAG or PST-AAA-FLAG and  $\beta 4\text{GalT-I-myc}$  or  $\beta 4\text{GalT-II-myc}$ . PST-FLAG or PST-AAA-FLAG was detected with anti-FLAG pAb (B, E, H, and K), and Alexa 546-conjugated secondary antibodies.  $\beta 4\text{GalT-myc}$  (I and II) was detected with anti-Myc mAb (C, F, I, and L) and Alexa 488-conjugated secondary antibodies. D, G, J, and M, overlaid images. Bar, 10  $\mu\text{m}$ . CT, cytoplasmic tail, TM, transmembrane domain.

of the dibasic motif (K/R)(X)(K/R) in PST. PST is also localized to the Golgi apparatus, as confirmed by the co-localization of PST-FLAG with  $\beta 4\text{GalT-I}$ , and -II-myc in the Golgi (Fig. 5, B–G). As expected, the altered distribution of PST-AAA-FLAG was observed as shown in Fig. 5, H and K, and also in [supplemental Fig. 3, G and J](#). The distribution of PST-AAA is slightly

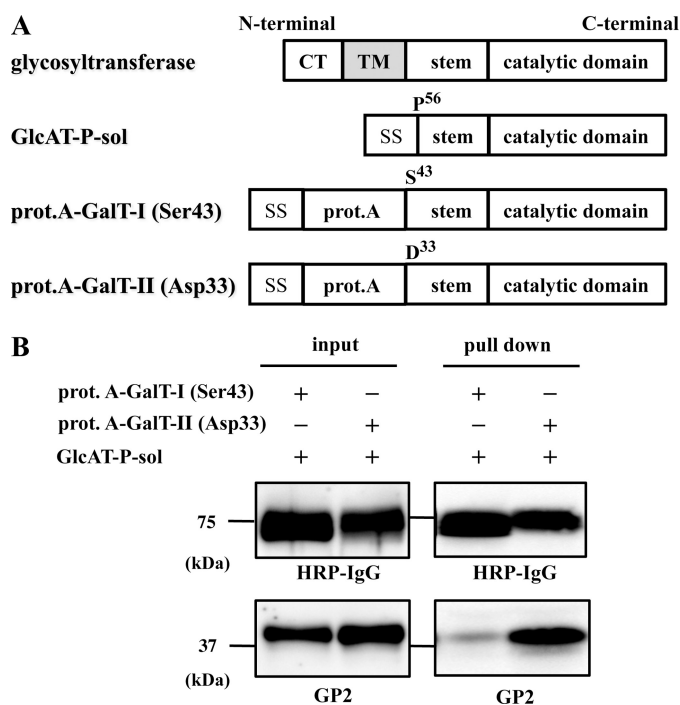


**FIGURE 6. Pulldown assays using soluble forms of  $\text{GlcAT-P-sol}$ ,  $\text{prot.A-GalT-I}$ , and  $\text{prot.A-GalT-II}$ .** A, schematic diagrams of  $\text{GlcAT-P-sol}$ ,  $\text{prot.A-GalT-I}$  (Ser-43), and  $\text{prot.A-GalT-II}$  (Asp-33). SS, signal sequence. B, culture medium of N2a cells transiently expressing  $\text{GlcAT-P-sol}$  and  $\text{prot.A-GalT-I}$  (Ser-43) or  $\text{prot.A-GalT-II}$  (Asp-33) was incubated with IgG-Sepharose TM6 Fast Flow (pulldown), subjected to SDS-PAGE, and Western-blotted with HRP-conjugated normal rabbit IgG or GP2 pAb. To examine the level of each protein, the culture medium was directly subjected to SDS-PAGE and then Western-blotted with HRP-conjugated normal rabbit IgG or GP2 pAb (input). CT, cytoplasmic tail, TM, transmembrane domain.

different from  $\text{GlcAT-P-AAA}$ , *i.e.* PST-AAA was detected not only in ER but in Golgi, suggesting that the effect of the mutation of dibasic motif on ER distribution varies by an individual glycosyltransferase as described previously (32). However, the altered distribution of PST-AAA did not perturb the Golgi-based localization of  $\beta 4\text{GalT-I}$  and -II-myc (Fig. 5, I, J, L, and M, and also see [supplemental Fig. 3, H, I, K, and L](#)). These results revealed that  $\beta 4\text{GalT-I}$  and -II do not associate with PST, supporting our idea that  $\beta 4\text{GalT-II}$  and  $\text{GlcAT-P}$  form a specific complex.

**Interaction between  $\text{GlcAT-P}$  and  $\beta 4\text{GalT-II}$  through Their Luminal Domains**—Glycosyltransferases, such as  $\text{GlcAT-P}$  and  $\beta 4\text{GalT}$ , are type II transmembrane proteins with a short cytoplasmic tail, a hydrophobic single-pass transmembrane domain, a stem region, and a catalytic domain (Fig. 6A) (36). We previously reported that  $\text{GlcAT-P}$  and  $\text{HNK-1ST}$  formed an enzyme complex through their catalytic domains in the Golgi lumen (37). Thus, we examined whether  $\text{GlcAT-P}$  and  $\beta 4\text{GalT-II}$  also form a complex via their Golgi luminal domains. We constructed an expression vector encoding the luminal domain of  $\text{GlcAT-P}$  downstream of the insulin signal sequence ( $\text{GlcAT-P-sol}$ ). Similarly, expression vectors for luminal domains of  $\beta 4\text{GalT-I}$  and -II fused with the signal sequence and protein A ( $\text{prot.A-GalT-I}$  (Ser-43) and  $\text{prot.A-GalT-II}$  (Asp-33), respectively) were constructed (Fig. 6A). The culture medium of N2a cells expressing  $\text{GlcAT-P-sol}$  and  $\text{prot.A-GalT-I}$  (Ser-43) or -II (Asp-33) was incubated with IgG-Sephar-

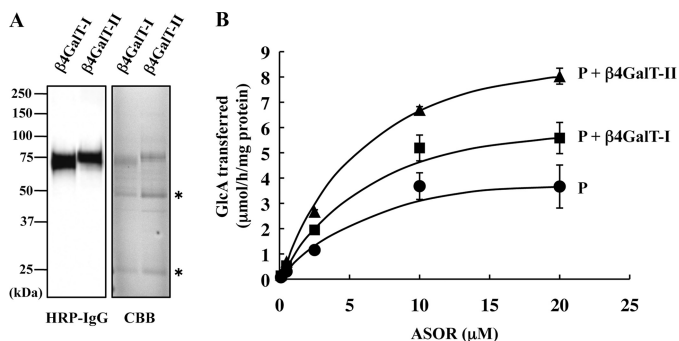


**FIGURE 7. Effect of the co-presence of  $\beta 4\text{GalT-II}$  on the *in vitro* glucuronyltransferase reaction of  $\text{GlcAT-P}$ .** A, prot.A-GalT-I (Ser-43) ( $\beta 4\text{GalT-I}$ ) or -II (Asp-33) ( $\beta 4\text{GalT-II}$ ) was expressed in COS-1 cells and purified from the culture media. The purified enzymes were subjected to Western blotting with HRP-conjugated rabbit IgG and Coomassie Brilliant Blue (CBB) staining. Asterisks indicate heavy and light chains of immunoglobulin derived from human IgG Sepharose. B, rate of glucuronyltransferase reaction of FLAG-P was measured in the absence of  $\beta 4\text{GalT}$ s (P), or in the presence of prot.A-GalT-I (Ser-43) (P +  $\beta 4\text{GalT-I}$ ) or prot.A-GalT-II (Asp-33) (P +  $\beta 4\text{GalT-II}$ ) using different concentrations of ASOR as substrates. All experiments were employed in triplicate, and error bars indicate S.E.

ose beads to pull down the prot.A-tagged enzymes. Subsequent Western blotting was conducted with HRP-conjugated IgG and anti-GlcAT-P pAb (GP2) to detect prot.A-fused enzymes and GlcAT-P, respectively. As shown in Fig. 6B, GlcAT-P-sol was highly co-precipitated with prot.A-GalT-II compared with prot.A-GalT-I, indicating that Golgi luminal domains are enough to form the enzyme complex. To narrow down the binding region of Golgi luminal domains of  $\beta 4\text{GalT}$ s, we also constructed expression vectors for catalytic domains of  $\beta 4\text{GalT-I}$  and -II fused with the signal sequence and protein A (prot.A-GalT-Icat (Leu-129) and prot.A-GalT-IIcat (Ile-91), respectively) and performed pulldown assay as described above. However, neither prot.A-GalT-Icat (Leu-129) nor prot.A-GalT-IIcat (Ile-91) interacts with GlcAT-P-sol (data not shown), suggesting that the deleted stem region are necessary for the specific binding of GlcAT-P and  $\beta 4\text{GalT-II}$ . Therefore, prot.A-GalT-I (Ser-43) and prot.A-GalT-II (Asp-33) were used for the following kinetic analysis of GlcAT-P.

**Kinetic Analysis of  $\text{GlcAT-P}$** —Next, to investigate whether or not a specific association of  $\beta 4\text{GalT-II}$  affects GlcAT-P activity, we examined the dependence of the rate of the glucuronyltransferase reaction on the concentration of ASOR as a glycoprotein acceptor in the presence or absence of  $\beta 4\text{GalT-I}$  or  $\beta 4\text{GalT-II}$ . For this kinetic analysis, we used FLAG-tagged human GlcAT-P (from Thr-58 to the C terminus, FLAG-P) expressed in *E. coli*. The method for expression and purification of FLAG-P had been already established (29). Human GlcAT-P is highly homologous to mouse GlcAT-P, especially 99.3% of amino acids are identical in the region we used (Thr-58 to C terminus). prot.A-GalT-I (Ser-43) and prot.A-GalT-II (Asp-33) were purified from culture media of COS-1 cells that had been transfected with their expression vectors as shown in Fig. 7A. The rate of glucuronyltransferase reaction of FLAG-P in the absence of prot.A-GalTs was compared with that in the presence of prot.A-GalT-I (Ser-43) or prot.A-GalT-II (Asp-33) using different concentrations of ASOR. As shown in Fig. 7B, the rate of FLAG-P reaction was increased depending on the concentration of ASOR and enhanced in the presence of GalT-I

**TABLE 1**  
Kinetic parameters of GlcAT-P

	$K_m$	$V_{max}$	$k_{cat}$	$k_{cat}/K_m$	Relative $k_{cat}/K_m$
	$\mu\text{M}$	$\mu\text{mol/h/mg}$	$\text{s}^{-1}$	$\mu\text{M}^{-1}\text{s}^{-1}$	-fold
GlcAT-P	7.46	4.90	0.0545	7.30	1
GlcAT-P + $\beta 4\text{GalT-I}$	6.62	7.53	0.0837	12.6	1.73
GlcAT-P + $\beta 4\text{GalT-II}$	6.09	9.86	0.110	18.0	2.47

or -II. The data were analyzed by means of Lineweaver-Burk plotting, and the kinetic parameters were then determined (Table 1). Apparent  $V_{max}$  value was increased about 2-fold, and the apparent  $K_m$  value was slightly decreased by  $\beta 4\text{GalT-II}$ . Thus,  $\beta 4\text{GalT-II}$  resulted in an approximate 2.5-fold increase in the catalytic efficiency  $k_{cat}/K_m$  of FLAG-P. To our surprise,  $\beta 4\text{GalT-I}$ , which does not associate with GlcAT-P, also enhanced the catalytic efficiency  $k_{cat}/K_m$  about 1.7-fold. However, the catalytic efficiency in the presence of  $\beta 4\text{GalT-II}$  is still higher than that of  $\beta 4\text{GalT-I}$ . These results suggest that the enzyme complex of GlcAT-P and  $\beta 4\text{GalT-II}$  is indeed capable of facilitating the expression of HNK-1.

**Enhanced HNK-1 Biosynthesis by Enzyme Complex in N2a Cells**—To determine the effect of the interaction on HNK-1 carbohydrate production in cells, a Western blot analysis was performed with the M6749 mAb. This mAb recognizes nonsulfated HNK-1 carbohydrate (GlcA $\beta$ 1-3Gal $\beta$ 1-4GlcNAc) (38), and N2a cells do not express endogenous GlcAT-P or HNK-1 carbohydrate (Fig. 8A, 1st lane). By employing this antibody, we can examine the level of nonsulfated HNK-1 carbohydrate, which was produced by GlcAT-P (Fig. 8A, 2nd lane). GlcAT-P and  $\beta 4\text{GalT-I}$  or -II-myc were co-expressed in N2a cells, and then cell lysates were subjected to SDS-PAGE and Western-blotted with the M6749 mAb, GP2 pAb, and anti-Myc mAb. As shown in Fig. 8A, M6749 immunoreactivity was increased when co-expressed with  $\beta 4\text{GalT-I}$  and -II-myc despite the comparable expression of GlcAT-P (compare 2nd lane with 3rd and 4th lanes), probably because of the increased amount of *N*-acetyllactosamine, which can be utilized as an acceptor by GlcAT-P. Intriguingly, however, M6749 immunoreactivity was increased more when GlcAT-P was co-expressed with  $\beta 4\text{GalT-II-myc}$  than with  $\beta 4\text{GalT-I-myc}$  (Fig. 8A, compare 3rd with 4th lane). To confirm these results, we quantitated two bands (see Fig. 8A, band 1 and 2) by means of densitometric analysis using image analysis software ImageGauge (FujiFilm). As shown in Table 2, co-expression of GlcAT-P and  $\beta 4\text{GalT-II-myc}$  caused about 3-fold (see Fig. 8A, bands 1 and 2) increases in M6749 immunoreactivity compared with that of GlcAT-P, and a 2-(band 1) or 1.4-fold (band 2) increase compared with that of GlcAT-P and  $\beta 4\text{GalT-I-myc}$ . These suggest that  $\beta 4\text{GalT-II}$  is better able to promote HNK-1 biosynthesis by associating with GlcAT-P. We carried out a similar analysis with immunoprecipitated NCAM, which is endogenously expressed in N2a cells. As shown in Fig. 8B, the highest expression of the M6749 epitope was observed when GlcAT-P was co-expressed with  $\beta 4\text{GalT-II-myc}$ . These results suggest that the complex of GlcAT-P and  $\beta 4\text{GalT-II}$  contributes to the enhancement of HNK-1 synthesis.

## Complex of $\beta 4$ GalT-II and GlcAT-P in HNK-1 Biosynthesis

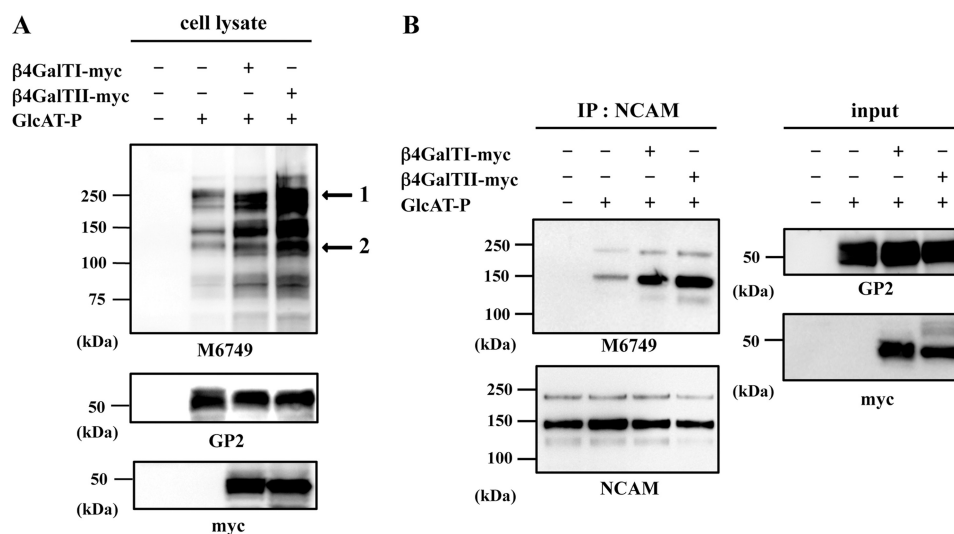


**FIGURE 8. Effect of the enzyme complex on HNK-1 expression in N2a cells.** *A*, lysates of N2a cells transiently expressing GlcAT-P,  $\beta 4$ GalT-I-myc, or  $\beta 4$ GalT-II-myc were subjected to SDS-PAGE and then Western blotted with M6749 mAb, GP2 pAb, or anti-Myc mAb. Arrows indicate bands used for quantification by densitometric analyses. *B*, lysates of N2a cells transiently expressing GlcAT-P and  $\beta 4$ GalT-I-myc or  $\beta 4$ GalT-II-myc were immunoprecipitated (IP) with anti-NCAM mAb and subjected to SDS-PAGE and then Western-blotted with M6749 mAb or anti-NCAM mAb.

**TABLE 2**  
Quantitative analysis of the effect of the enzyme complex

	Mock	GlcAT-P	GlcAT-P + $\beta 4$ GalT-I-myc	GlcAT-P + $\beta 4$ GalT-II-myc
<b>Band 1</b>				
Intensity (a.u.) <sup>a</sup>	0	0.48	0.77	1.53
-Fold		1.00	1.60	3.20
<b>Band 2</b>				
Intensity (a.u.)	0	0.21	0.43	0.60
-Fold		1.00	2.03	2.86

<sup>a</sup> The immunoreactivity with M6749 mAb was calculated and normalized to GlcAT-P expression and is shown as intensity in arbitrary units (a.u.).

## DISCUSSION

The  $\beta 4$ GalT family has seven members, but the biological roles have not been fully understood. We recently reported that  $\beta 4$ GalT-II-deficient mice showed a marked reduction in levels of HNK-1 carbohydrate and impaired spatial memory, and the phenotypes are similar to those of GlcAT-P-deficient mice (19). Moreover,  $\beta 4$ GalT-II is highly expressed in the brain although  $\beta 4$ GalT-I is ubiquitous (39). These findings suggest intrinsic roles *in vivo*, although  $\beta 4$ GalT-I and -II show the highest sequence similarity among  $\beta 4$ GalTs. Analyses using these gene-deficient mice revealed that  $\beta 4$ GalT-II is crucial to the production of HNK-1, but the underlying mechanism was not elucidated. In this study, we produced evidence that  $\beta 4$ GalT-II physically associates with GlcAT-P (Figs. 2 and 3) probably through the luminal stem domain of  $\beta 4$ GalT-II. Considering the similar domain organizations and molecular sizes of GlcAT-P and  $\beta 4$ GalT-II, the stem domain of GlcAT-P may also be involved in this interaction. Because we had revealed that GlcAT-P bound to HNK-1ST through the catalytic region (37),  $\beta 4$ GalT-II seems not to compete with HNK-1ST for the binding to GlcAT-P; rather, these three enzymes may simultaneously form a large functional complex to synthesize HNK-1 efficiently in living cells. Actually, we revealed that  $\beta 4$ GalT-II is capable of increasing the catalytic efficiency  $k_{cat}/K_m$  of the GlcAT-P catalytic reaction using *in vitro* enzyme assay system (Fig. 7). Also in N2a cells, the co-expression of  $\beta 4$ GalT-II and

GlcAT-P enhanced HNK-1 biosynthesis (Fig. 8). These results suggest that HNK-1 expression is regulated by the interaction of these two enzymes.

We found that both  $\beta 4$ GalT-I- and -II-deficient mice showed normal levels of *N*-acetylglucosamine on *N*-glycans, indicating that several  $\beta 4$ GalTs actually contribute to galactosylation in the brain. The specific loss of HNK-1 in  $\beta 4$ GalT-II-deficient mice can be explained in several ways. The present analysis suggests that  $\beta 4$ GalT-II is not the only enzyme for *N*-acetylglucosamine synthesis in HNK-1-expressing cells because *N*-acetylglucosamine is likely expressed at normal levels in  $\beta 4$ GalT-II knock-out mice even on NCAM. Our experiment showed that  $\beta 4$ GalT-II does not specialize in the galactosylation of HNK-1-expressing molecules such as NCAM by recognizing their polypeptide backbones, because the galactosylation of NCAM is unlikely to be impaired in  $\beta 4$ GalT-II knock-out mice.  $\beta 4$ GalT-II might act on a specific *N*-glycosylation site or specific branch of *N*-glycan that is preferentially modified further by GlcAT-P. We demonstrated here that simply the presence of *N*-acetylglucosamine or GlcAT-P is not sufficient for HNK-1 biosynthesis and that both *N*-acetylglucosamines synthesized by  $\beta 4$ GalT-II and GlcAT-P are required. Although  $\beta 4$ GalT-II is involved in HNK-1 biosynthesis, this enzyme is not a chaperone-like molecule for GlcAT-P, because a recombinant GlcAT-P from *E. coli* was fully active without  $\beta 4$ GalT-II *in vitro* (29). Rather, we speculate that  $\beta 4$ GalT-II would be in a specialized complex with GlcAT-P in a specific Golgi compartment to cooperatively catalyze their transfer reactions for HNK-1 synthesis on specific glycoproteins.

To our surprise,  $\beta 4$ GalT-I also had the potential to activate HNK-1 biosynthesis (Fig. 8), even though its effect was weaker than  $\beta 4$ GalT-II. This result could be explained by the overproduction of *N*-acetylglucosamine residues by  $\beta 4$ GalT-I overexpression even without enzyme-enzyme interaction. Meanwhile, our *in vitro* analysis also showed that  $\beta 4$ GalT-I weakly activated GlcAT-P catalytic activity (Fig. 7). Although we could not detect the interaction between GlcAT-P and  $\beta 4$ GalT-I in



cell-based co-immunoprecipitation assays, weaker binding was observed in pulldown assays (Fig. 6B). These results suggest that  $\beta$ 4GalT-I could compensate for the loss of HNK-1 biosynthesis in  $\beta$ 4GalT-II-deficient cells if it could be overexpressed. Because HNK-1 expression almost disappeared in the  $\beta$ 4GalT-II-deficient brain, it suggests that the levels of other  $\beta$ 4GalTs in HNK-1-expressing cells may be under the levels that are required for compensation for the loss of  $\beta$ 4GalT-II.

We previously reported that  $\beta$ 4GalT-I- and -II-deficient mice showed the same level of PSA expression as wild-type mice, indicating that the biosynthesis of PSA does not depend on these enzymes (19, 20). Also, we found that PST does not associate with  $\beta$ 4GalT-I or -II (Fig. 4). Regarding the biosynthesis of PSA, another  $\beta$ 4GalT may be associated with polysialyltransferase to specifically synthesize the inner structure of PSA. Alternatively, polysialyltransferase may not distinguish between the inner *N*-acetylglucosamines synthesized by several  $\beta$ 4GalTs. Other  $\beta$ 4GalTs could compensate for the loss of deficiency of a given  $\beta$ 4GalT. Moreover, acidic amino acid residues in the fibronectin type III domain adjacent to the fifth Ig domain of NCAM, which has *N*-glycosylation sites attaching to PSA, were reported to be required for polysialylation (40). PSA biosynthesis would be mainly dependent on the polypeptide backbone of NCAM rather than the enzyme responsible for production of the inner *N*-acetylglucosamine. It is indicated that the biosynthesis of PSA is considerably different from that of HNK-1, despite some common features between these two neural glycans expressed on NCAM.

In recent years, many groups have reported that enzyme complexes of glycosyltransferases have enhanced catalytic activities. Seko and Yamashita (5) showed that a complex of  $\beta$ 3GnT2 and  $\beta$ 3GnT8 produced more poly-*N*-acetylglucosamine. Our previous study demonstrated that GlcAT-P interacts with HNK-1ST, and the interaction enhances the enzymatic activity of HNK-1ST (37). Also, it has been reported that the activities of some glycosyltransferases are regulated through interaction with nonglycosyltransferases. For example, GnT-I activity was inhibited by interaction with GnT-I-IP (GnT-I inhibitory protein), resulting in the expression of high mannose-type *N*-glycans during spermatogenesis (41). T-synthase (C1 $\beta$ 3Gal-T) forms a complex with core 1  $\beta$ 3GalT-specific molecular chaperone, which functions as a specific chaperone. Core 1  $\beta$ 3GalT-specific molecular chaperone is essential for the T-synthase activity and synthesizing T-antigen (42). Actually, core 1  $\beta$ 3GalT-specific molecular chaperone is a factor responsible for Tn syndrome, a genetic disease involving a deficiency in T-antigen but no defect in T-synthase (43). In this study, we found that HNK-1 expression is not regulated simply by GlcAT-P but also by the interaction of the enzymes. Supporting this finding, the distribution of GlcAT-P mRNA did not completely match the pattern of HNK-1 expression in the brain. For example, HNK-1 antibody staining showed parasagittal stripes in the molecular layer in the cerebellum (44) because of HNK-1 carbohydrate expression on a limited population of Purkinje cells, whereas GlcAT-P mRNA is likely expressed in most Purkinje cells (45). It would be of interest to compare the distribution of  $\beta$ 4GalT-II mRNA and HNK-1 carbohydrate in the brain. Taken together, to understand the pre-

cise mechanisms of expression and proper functions of glycans, it is important to recognize that many glycosyltransferases form complexes *in vivo*.

HNK-1 carbohydrate has an important role in synaptic plasticity and spine morphogenesis in the nervous system (14, 15). These functions are based on its specific expression on certain carriers such as NCAM and GluR2, which is a subunit of the  $\alpha$ -amino-3-hydroxy-5-methylisoxazole propionate-type glutamate receptor. It should be noted that another subunit, GluR1, which forms a complex with GluR2 to make a functional  $\alpha$ -amino-3-hydroxy-5-methylisoxazole propionate receptor *in vivo*, is not modified with HNK-1 (46) even if several complex-type *N*-glycans are expressed on GluR1. This indicates that HNK-1 carbohydrate greatly contributes to the specific function of GluR2, but the underlying mechanism of this selective modification is poorly understood. It could be involved in the selective modification to form the complex of  $\beta$ 4GalT-II and GlcAT-P. As well as HNK-1 carbohydrate, many glycans are expressed on specific target proteins, thereby regulating their functions. Thus, it is of great interest to study the mechanisms by which the functions of individual glycosyltransferases are regulated to produce glycoconjugates.

## REFERENCES

- Ohtsubo, K., and Marth, J. D. (2006) *Cell* **126**, 855–867
- Lowe, J. B., and Marth, J. D. (2003) *Annu. Rev. Biochem.* **72**, 643–691
- Sugimoto, I., Futakawa, S., Oka, R., Ogawa, K., Marth, J. D., Miyoshi, E., Taniguchi, N., Hashimoto, Y., and Kitazume, S. (2007) *J. Biol. Chem.* **282**, 34896–34903
- Seko, A. (2006) *Trends Glycosci. Glycotechnol.* **18**, 209–230
- Seko, A., and Yamashita, K. (2008) *J. Biol. Chem.* **283**, 33094–33100
- Lee, P. L., Kohler, J. J., and Pfeffer, S. R. (2009) *Glycobiology* **19**, 655–664
- Schwartz, G. A., Jungalwala, F. B., Chou, D. K., Boyer, A. M., and Yamamoto, M. (1987) *Dev. Biol.* **120**, 65–76
- Yoshihara, Y., Oka, S., Watanabe, Y., and Mori, K. (1991) *J. Cell Biol.* **115**, 731–744
- Voshol, H., van Zuylen, C. W., Orberger, G., Vliegthart, J. F., and Schachner, M. (1996) *J. Biol. Chem.* **271**, 22957–22960
- Oka, S., Terayama, K., Kawashima, C., and Kawasaki, T. (1992) *J. Biol. Chem.* **267**, 22711–22714
- Terayama, K., Oka, S., Seiki, T., Miki, Y., Nakamura, A., Kozutsumi, Y., Takio, K., and Kawasaki, T. (1997) *Proc. Natl. Acad. Sci. U.S.A.* **94**, 6093–6098
- Seiki, T., Oka, S., Terayama, K., Imiya, K., and Kawasaki, T. (1999) *Biochem. Biophys. Res. Commun.* **255**, 182–187
- Bakker, H., Friedmann, I., Oka, S., Kawasaki, T., Nifant'ev, N., Schachner, M., and Mantei, N. (1997) *J. Biol. Chem.* **272**, 29942–29946
- Yamamoto, S., Oka, S., Inoue, M., Shimuta, M., Manabe, T., Takahashi, H., Miyamoto, M., Asano, M., Sakagami, J., Sudo, K., Iwakura, Y., Ono, K., and Kawasaki, T. (2002) *J. Biol. Chem.* **277**, 27227–27231
- Morita, I., Kakuda, S., Takeuchi, Y., Kawasaki, T., and Oka, S. (2009) *Neuroscience* **164**, 1685–1694
- Kizuka, Y., Tonoyama, Y., and Oka, S. (2009) *J. Biol. Chem.* **284**, 9247–9256
- Lo, N. W., Shaper, J. H., Pevsner, J., and Shaper, N. L. (1998) *Glycobiology* **8**, 517–526
- Hennet, T. (2002) *Cell. Mol. Life Sci.* **59**, 1081–1095
- Yoshihara, T., Sugihara, K., Kizuka, Y., Oka, S., and Asano, M. (2009) *J. Biol. Chem.* **284**, 12550–12561
- Kido, M., Asano, M., Iwakura, Y., Ichinose, M., Miki, K., and Furukawa, K. (1998) *Biochem. Biophys. Res. Commun.* **245**, 860–864
- Almeida, R., Amado, M., David, L., Lavery, S. B., Holmes, E. H., Merckx, G., van Kessel, A. G., Rygaard, E., Hassan, H., Bennett, E., and Clausen, H. (1997) *J. Biol. Chem.* **272**, 31979–31991

## Complex of $\beta$ 4GalT-II and GlcAT-P in HNK-1 Biosynthesis

22. Guo, S., Sato, T., Shirane, K., and Furukawa, K. (2001) *Glycobiology* **11**, 813–820
23. Rutishauser, U. (2008) *Nat. Rev. Neurosci.* **9**, 26–35
24. Mühlenhoff, M., Eckhardt, M., and Gerardy-Schahn, R. (1998) *Curr. Opin. Struct. Biol.* **8**, 558–564
25. Kudo, M., Kitajima, K., Inoue, S., Shiokawa, K., Morris, H. R., Dell, A., and Inoue, Y. (1996) *J. Biol. Chem.* **271**, 32667–32677
26. Asano, M., Furukawa, K., Kido, M., Matsumoto, S., Umesaki, Y., Kochibe, N., and Iwakura, Y. (1997) *EMBO J.* **16**, 1850–1857
27. Kakuda, S., Sato, Y., Tonoyama, Y., Oka, S., and Kawasaki, T. (2005) *Glycobiology* **15**, 203–210
28. Qasba, P. K., Ramakrishnan, B., and Boeggeman, E. (2008) *Curr. Drug Targets* **9**, 292–309
29. Kakuda, S., Oka, S., and Kawasaki, T. (2004) *Protein Expr. Purif.* **35**, 111–119
30. Kruse, J., Mailhammer, R., Wernecke, H., Faissner, A., Sommer, I., Goridis, C., and Schachner, M. (1984) *Nature* **311**, 153–155
31. Nilsson, T., Hoe, M. H., Slusarewicz, P., Rabouille, C., Watson, R., Hunte, F., Watzele, G., Berger, E. G., and Warren, G. (1994) *EMBO J.* **13**, 562–574
32. Giraudo, C. G., and Maccioni, H. J. (2003) *Mol. Biol. Cell* **14**, 3753–3766
33. Eckhardt, M., Mühlenhoff, M., Bethe, A., Koopman, J., Frosch, M., and Gerardy-Schahn, R. (1995) *Nature* **373**, 715–718
34. Kojima, N., Yoshida, Y., and Tsuji, S. (1995) *FEBS Lett.* **373**, 119–122
35. Nakayama, J., and Fukuda, M. (1996) *J. Biol. Chem.* **271**, 1829–1832
36. Breton, C., Mucha, J., and Jeanneau, C. (2001) *Biochimie* **83**, 713–718
37. Kizuka, Y., Matsui, T., Takematsu, H., Kozutsumi, Y., Kawasaki, T., and Oka, S. (2006) *J. Biol. Chem.* **281**, 13644–13651
38. Tagawa, H., Kizuka, Y., Ikeda, T., Itoh, S., Kawasaki, N., Kurihara, H., Onozato, M. L., Tojo, A., Sakai, T., Kawasaki, T., and Oka, S. (2005) *J. Biol. Chem.* **280**, 23876–23883
39. Nakamura, N., Yamakawa, N., Sato, T., Tojo, H., Tachi, C., and Furukawa, K. (2001) *J. Neurochem.* **76**, 29–38
40. Mendiratta, S. S., Sekulic, N., Lavie, A., and Colley, K. J. (2005) *J. Biol. Chem.* **280**, 32340–32348
41. Huang, H. H., and Stanley, P. (2010) *J. Cell Biol.* **190**, 893–910
42. Ju, T., and Cummings, R. D. (2002) *Proc. Natl. Acad. Sci. U.S.A.* **99**, 16613–16618
43. Ju, T., and Cummings, R. D. (2005) *Nature* **437**, 1252
44. Marzban, H., Sillitoe, R. V., Hoy, M., Chung, S. H., Rafuse, V. F., and Hawkes, R. (2004) *J. Neurocytol.* **33**, 117–130
45. Inoue, M., Kato, K., Matsuhashi, H., Kizuka, Y., Kawasaki, T., and Oka, S. (2007) *Brain Res.* **1179**, 1–15
46. Morita, I., Kakuda, S., Takeuchi, Y., Itoh, S., Kawasaki, N., Kizuka, Y., Kawasaki, T., and Oka, S. (2009) *J. Biol. Chem.* **284**, 30209–30217